Quantum Bio-inspired Invariant Object Recognition Model on System-on-a-Chip (SoC)

Loo Chu Kiong
Faculty of Engineering and Technology
Multimedia University
Melaka, Malaysia
ckloo@mmu.edu.my

Teh Joo Peng
Faculty of Engineering and Technology
Multimedia University
Melaka, Malaysia
teh_joo_peng@yahoo.com

Abstract— **This paper presents the first attempt of designing a physical quantum-like 'brain' for humanoid and experimentally proves a 2D invariant object recognition model inspired by the image processing along the human visual pathway: retina, lateral geniculate nucleus (LGN) and primary visual cortex (V1). It also describes storing the output of the model in quantum holographic memory (a hologram) and the method to reconstruct the visual representation. The work is implemented as system-on-a-chip in field-programmable gate array (FPGA).**

Keywords—**Biological-inspired vision, System-on-a-chip, invariant object recognition, FPGA design.**

I. INTRODUCTION

Object recognition is a popular area of research in machine vision. Its application in humanoid robots enables them to understand the dynamics of scene and to pursue a higher level of cognitive task to interact with real-world environment. By definition humanoid robot is a robot with its overall appearance based on human body, so by implying, a true humanoid brain should be a processing unit that resembles the biological model of human brain. This paper describes the humanoid brain implementation of a bio-inspired 2D invariant object recognition model on system-on-a-chip (SoC).

Currently, the most studied part of human brain is the human visual system. Research in neuroscience has led to a more extensive knowledge of the computational properties of individual cells and their interactions in the visual pathway. It has provided a basis of image processing derived from the structure and function of real brain. This has spawned several bio-inspired object recognition model [1][2][3] that have described and simulated mathematical formulation of computation performed in visual pathway, from retina to primary visual cortex, to achieve invariant object recognition.

Bio-inspired model provides relative good accuracy but the heavy computation resulted in low performance when executed in general processor. Thus there are attempts to design and develop customized hardware that are strongly inspired by biological neural processing. For example, [4] has designed on FPGA the biological processing of retina; [5] has design on FPGA the interactions between areas in brain. A field-programmable gate array (FPGA), which allows custom digital circuits to be programmed, is usually the choice for custom hardware design. It allows optimized application performance through real hardware parallel processing, as opposed to general processor which provides time-multiplex parallel processing.

The bio-inspired invariant object recognition models proposed by [1][2][3] are only simulation. This paper describes the implementation of similar model in a hardware humanoid brain, but the model proposed in this paper differs as it combines Quantum Associative Networks for object recognition. Unlike [4], [5] who implemented their custom hardware purely from VHDL, this paper instead describes integrating a general processor with custom hardware, i.e. a system-on-a-chip. This paper is not intended to propose a better or faster hardware implementation of object recognition but merely to present the work done to date.

Section 2 provides the biological and mathematical foundation of the 2D invariant object recognition. In section 3, the overall architectural approach for the model humanoid implementation is presented. Section 4 presents the result..

II. BIO-INSPIRED MODEL

A. Background

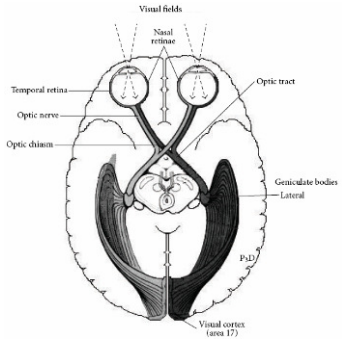

Figure 1. Visual pathway, obtained from [7]

Human visual system is part of the brain. Over the course of evolution, it has grown out of the brain to provide front view visual input to the back of the brain. This paper will use a simplified view of human vision, in which light coming from the visual field is sampled by the photoreceptors at retina, outputs to lateral geniculate nucleus (LGN), which then relays the visual signal to primary visual cortex (V1). See Figure 1. In

reality the visual pathway is not uni-directionally feedforward, where there are feedback nerves from the V1 to LGN ten times as much as feedforward nerves [6], however that is beyond the discussion in this paper.

B. Retino-Cortical Mapping

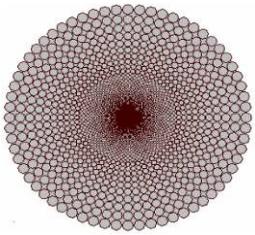

Figure 2. Distribution of retinal receiver, a foveated view, obtained from [4].

Based on experiment maps of the retina to visual cortex projection of the cat and various primates [8], [9] proposed that the projection of human retina to visual cortex can be approximated by log-polar mapping function $\boldsymbol{w = \log(z+a)}$, where z and w are complex numbers defining points in retina and visual cortex space respectively. The real number "a" takes care of the deviation of the exact logarithm mapping from the center of retina image plane. This is to say that in the human vision system the receptors in the retina are spatially distributed, with a growing density toward the centre of the visual field, denominated fovea, and with a falling density from the fovea to the periphery of the visual field. This kind of vision is called "spatially variant perception", and it carries out a selective sampling, on the visual field [4]. See Figure 2. If an image is at center of the image plane, a = 0, the exact log-polar mapping converts rotation and scaling in the image plane into translation in the log-polar plane. This means, the same object of different size or rotation has patterns mapping in the log-polar plane that are of the same shape but at different position. Schwartz proposed that this principle of logarithm mapping as a possible model for scale- and rotation invariant pattern representation in the human visual system [9].

In cat's primary visual cortex, [11] found simple and complex cells that are selective to intensity changes in specific orientation. The orientation selectivity of cells is accomplished through spatial summation of the inputs from LGN. Reference [12] proposed the use of Gabor filters to model the orientation selective receptive fields of simple cells in the visual cortex of some mammals. In early 1980's a number of researchers suggested Gabor filters (Gaussian modulated sinusoids) as models of the receptive fields of simple cells in visual cortex [13][14][15].

C. Retina-LGN-Visual Cortex Visual Pathway

Thus far, LGN is viewed as a relay station and it merely relays information from ganglion cells in the retina to visual cortex [6]. But [1] argue that apart from merely a relay station, LGN applies Difference of Gaussian (DOG) filter to reduce the details of visual information. In this paper, it assumes LGN performs DOG of the input image before relaying it to visual cortex. This DOG filter is special in such that its variance increases linearly when it move away from the center of visual field. It is challenging to use this varying DOG filter with convolution since conventionally the filter mask is constant. This issue is solved by applying Laplacian of Gaussian filter on the log-polar plane, because application of a small variance constant spatial filter in the log-polar domain is approximately equivalent to the application of a space-variant filter of similar shape in the object domain. Thus combination of log-polar transform and Laplacian of Gaussian filter yields DOG [10].

Hubel [11] also discovered that the orientation selectivity of simple cells in a column perpendicular to V1 surface remained almost constant, and the orientation selectivity varies systematically along the surface of V1. This kind of cell arrangement is referred to as hypercolumn. See Figure 3. This lays the idea for convolving input from LGN with Gabor filters of different angle in the model discussed later.

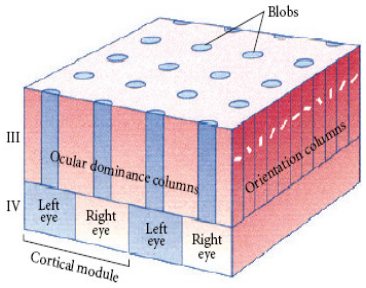

Figure 3. Hypercolumn in visual cortex, obtained from [16].

D. Quantum Neural Substrates of Vision

Apart from studying the physical property of neurons in visual cortex (V1), not much attention are focused on understanding the consciousness of the brain as consciousness itself cannot be probe nor measured, at least not for any instrument available in present day. To fill this gap, [14] proposed the brain as a hologram in which memory and perception are related to holographic principles. Assuming the brain is a hologram and thus using quantum holography, [17] has proposed a neuro-quantum computing model - the Quantum Associative Networks, for image storage and retrieval. Much like neural net theory, where image retrieval is reconstruction of an image from a database of many concrete images simultaneously stored in an associative memory, Quantum Associative Networks store many images of objects into quantum memory (a hologram). Image encoded into Gabor wavelets are similar to quantum wave packets [17], so it is natural that the output of the Gabor filtering in V1 hypercolumn can feed into Quantum Associative Networks. In addition, holonomic brain theory considers synapto-dendritic networks at the microscopic level. It believes image processing in V1 using Gabor wavelets are implemented by interacting dendritic polarization-fields [14].

III. MATHEMATICAL MODEL

The model in this paper is limited to the recognition of 2D object. It is assumed that there is only one object in the image while the surrounding is plain black background. The center of the object in the image is already adjusted to coincide with the

origin of the image, and additional translation preprocessing is not required.

A digitized image will undergo exact log-polar transformed so that the scale and rotation are transformed to translation in log-polar plane. The log-polar image is then filtered with Laplacian of Gaussian kernel. Then the filtered log-polar image undergoes 2D Fourier transform. The absolute value of the Fourier transform generates a translation-invariant spectrum of the log-polar plane, thus overall size and rotation invariance are achieved.

The spectrum will then be multiplied by frequency responses of Gabor filter with angular rotation from 0°, 1°, to 179° (multiplication in frequency domain is equivalent to convolution in spatial domain). The 180 spectrum results will be converted back to 180 spatial domain samples using inverse Fourier transform. Then the maximum value is chosen from every pixel of the 180 samples to generate a final spatial domain template. The template will be stored in quantum associative networks for future retrieval.

A. *Log-polar mapping*

Unlike the complex log-polar transform proposed by [9], implementation of log-polar transform in this paper deals only with real values. Given point in the log-polar space (ρ,θ), the equations to compute its cartesian coordinates (x,y) are:

$$x = \lambda^{\rho}.r_0.\cos(\theta)$$
$$y = \lambda^{\rho}.r_0.\sin(\theta)$$

log-polar to cartesian transformation

where: λ is the base of the logarithm.

r_0 is a scaling factor which define the size of the circle $\rho = 0$.

The inverse will be:

$$\rho = \log_{\lambda} \frac{\sqrt{x^2 + y^2}}{r_0}$$
$$\theta = \arctan \frac{y}{x}$$

Cartesian to log-polar transformation

The equation need to be modified to deal with digital images. Both Cartesian and log-polar domains have to be treated as discrete, so $(\boldsymbol{\rho},\boldsymbol{\theta})$ where $0 \le \boldsymbol{\rho} < P$ and $0 \le \boldsymbol{\theta} < \Theta$ represents the pixels in log-polar domain. In the same way, $(\boldsymbol{x},\boldsymbol{y})$ where $0 \le \boldsymbol{x} < X$ and $0 \le \boldsymbol{y} < Y$ represents the pixels in Cartesian domain. P is the total number of rings, Θ is the total number of pixels per ring, and X and Y are the horizontal and vertical sizes of the Cartesian image.

Since θ ranges in $0 \rightarrow \Theta$ and not in $0 \rightarrow 2\pi$, the range has to be scaled to cover a round angle:

$$\omega = \frac{2\pi\theta}{\Theta}$$

Leading to:

$$x = \lambda^{\rho}.r_0.\cos(\frac{2\pi\theta}{\Theta})$$
$$y = \lambda^{\rho}.r_0.\sin(\frac{2\pi\theta}{\Theta})$$

log-polar to cartesian transformation

and

$$\rho = \log_{\lambda} \frac{\sqrt{x^2 + y^2}}{r_0}$$
$$\theta = \frac{\Theta}{2\pi} \arctan \frac{y}{x}$$

cartesian to log-polar transformation

The logarithm base, λ is computed from the number of pixels per ring Θ:

$$\lambda = \frac{1 + \sin\frac{\pi}{\Theta}}{1 - \sin\frac{\pi}{\Theta}}$$

In this paper, P, Θ, X and Y are set to 256 pixels.

After log-polar transformation, I_{xy}^{Input} is mapped on to $I_{\rho\theta}^{Log}$ in (ρ,θ) Cartesian plane.

$$I^{Input}(x,y) \xrightarrow{\log-polar\,transform} I^{LOG}(\rho,\theta)$$

B. *Laplacian of Gaussian*

The log-polar mapping is then filtered with be the Laplacian of Gaussian kernel. The combination of log-polar transform and Laplacian of Gaussian filter yields DOG, or the "Mexican hat" function. In the present model, the circular symmetrical function [10] is used:

$$\nabla^2 G(x,y) = -\frac{1}{\pi\sigma^4}\left(1 - \frac{x^2 + y^2}{2\sigma^2}\right) e^{-\frac{x^2+y^2}{2\sigma^2}} \quad (1)$$

With $G(x,y) = -\frac{1}{2\pi\sigma^2} e^{-\frac{x^2+y^2}{2\sigma^2}}$

$\nabla^2 G$ is approximated on a 5×5 field and the σ is taken to be 0.5. The log-polar image is convolved with this filter. This resembles the functional properties of DOG filter (in lateral geniculate nucleus) whose diameter increases linearly from center of visual field. The combined operations can be expressed mathematically as follows:

$$I^{LGN}(\rho,\theta) = I^{LOG}(\rho,\theta) * \nabla^2 G_{\sigma} \quad (2)$$

C. *Gabor filters*

Gabor filter is the product of an elliptical Gaussian and a complex plane wave, resulting in 5 parameters. The first two parameters are the 2D-location of the receptive field's center, the third is the size of the receptive field, the fourth is the orientation of the boundaries separating excitatory and inhibitory regions, and the fifth is the symmetry. The fifth parameter is given in the standard Gabor transformation by the real and imaginary parts, i.e. by the phase, of the complex function representing it. There are three neurophysiological constraints that fix the relation between width, height, orientation and spatial frequency. The first constraint posits that the aspect ratio of the elliptical Gaussian envelope is 2:1. The second constraint postulates that the plane wave tends to have

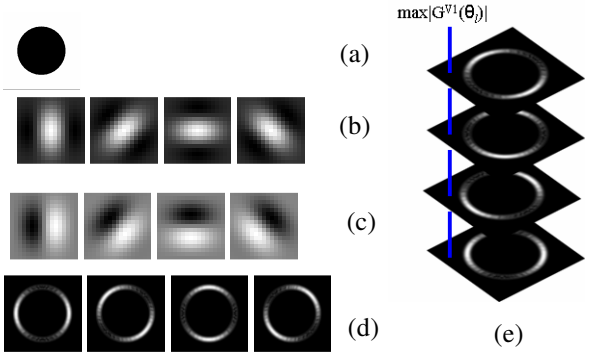

Figure 4. (a) sample input image (b)(C) real (even) and imaginary (odd) Gabor filters at 4 different angle (d) the modulus of the complex value convolution of the input image and Gabor filters (e) obtain the maximum at each point

its propagating direction along the short axis of the elliptical Gaussian. The third constraint assumes that the half-amplitude bandwidth of the frequency response is about 1 to 1.5 octaves along the optimal orientation. Reference [15] derived a family of 2D Gabor filter that satisfies all these neurophysiological constraints for simple cells and is given by

$$\Psi(x,y)=\frac{1}{\sqrt{2\pi}}e^{-(1/8)\left(4(x\cos\theta+y\sin\theta)^2+(-x\sin\theta+y\cos\theta)^2\right)}$$
$$\cdot\left[e^{i(\omega_0 x\cos\theta+\omega_0 y\sin\theta)}-e^{-\kappa^2/2}\right]$$
$$=\frac{1}{\sqrt{2\pi}}e^{-(1/8)\left(4(x\cos\theta+y\sin\theta)^2+(-x\sin\theta+y\cos\theta)^2\right)}\cdot$$
$$\left[\cos(\omega_0 x\cos\theta+\omega_0 y\sin\theta)-e^{-\kappa^2/2}+i\sin(\omega_0 x\cos\theta+\omega_0 y\sin\theta)\right] \quad (3)$$

In the above equation, $\theta=\theta_l=l\pi/L$ with L the number of angular rotation and l the index of rotation; L =180; ω_0 =1; $\kappa\approx\pi$ for a frequency bandwidth of one octave. In this form, the receptive fields at all levels cover the spatial domain in the same way. The neurons in the pools in $V1$ have receptive fields performing a Gabor wavelet transform. Let us denote $I^{V1}=I^{LGN}(x,y)$ be the sensory input activity to a pool of hypercolumns in $V1$. The sensory input activity to a pool of hypercolumns is therefore defined by the modulus of the complex valued convolution between the corresponding receptive fields and the image, i.e,

$$G^{V1}(x,y)=\left\|\Psi(x,y)*I^{LGN}(x,y)\right\| \quad (4)$$

In the above equation, the modulus is taken to get the energy model of complex cell. The Gabor energy is closely related to the local power spectrum [18] and local energy maps [19]. Edge and line features are signaled by local maximas in the local energy maps [Morrone and Burr, 88]. Gabor energy maps are generated for θ_l, l=1, 2, …, 179 and the maximum is chosen at each point (x,y) of the 180 Gabor energy maps, we obtain

$$G^{V1}(\bar{\theta})=\max_{\theta_{l=1,2,3,\ldots,179}}\left|G^{V1}(\theta_l)\right| \quad (5)$$

Figure X. summarizes the process above. The outputs of the complex cells, $G^{V1}(\bar{\theta})$ are used for subsequent quantum image processing.

D. Quantum Associative Networks

The quantum hologram G is given by the Hebb-equivalent expression:

$$G_{hj}=\sum_{k=1}^{P}\psi_h^k(\psi_j^k)* \quad (6)$$

Where *h* and *j* denote the pixel point at time *t* (*h*,*j*=1,...,N). ψ^k denotes the quantum wave. The asterisk denotes complex conjugate. After images are encoded into eigenstates (attractors) ψ^k in the quantum system by Eq. (6), an output eigenstates (say, the k_0^{th}) can be constructed by presenting a new input similar to the k_0^{th} stored one by:

$$\psi_h^{output}=\sum_{j=1}^{N}G_{hj}\psi_j^{input} \quad (7)$$

The Gabor wavelet patterns in V1, $\mathbf{G^{V1}}$ are equivalent to a family of quantum coherent states generated by Weyl-Heisenberg group [15]. Let us define the Dirac quantum notation: $|\cdot\rangle$ is a quantum eigenvector; $\langle\cdot|$ is its transpose and complex-or phase-conjugate. The first vector describes the state of a quantum system incorporating pixel-values, the second vector corresponds to the same state but with the opposite direction of wave-propagation. Recognition of an object, represented in V2, is realized by a Gabor-filtered quantum-encoded retinal input ($\mathbf{G^{V1}}=|\mathbf{\Psi}\rangle$). First we consider the Gabor-filtered quantum-encoded retinal input $\mathbf{G^{V1}}$ as a stationary geometrical pattern in three-dimensional space. A $\mathbf{G^{V1}}$ image $n\times m$ can be described as a set of $N=n\cdot m$ real numbers corresponding to the energy response value of each point, *i.e.* some vector $x\in R^N$. The *hyperspheres* $\left\{S^k:x\in R^{k+1},\|x\|=1\right\}$ and *projective spaces* (spaces of rays) $\left\{RP^k:[\mathbf{x}]\in\mathbf{R^{k+1}}/\mathbf{R^1},[\mathbf{x}]=[\lambda x_0,\lambda x_1,\ldots\lambda x_k];\mathbf{x}\neq 0,\lambda\neq 0\right\}$ are also can be used. For example, in cases of grey image, we can multiply all intensities on the same nonzero positive value

and the image does not change. Due to such invariance we can use only vectors with unit length and space of images is subspace of the sphere $\mathbf{S}^{N-1}$. In addition, to ensure the *homogeneous* distribution of images in the space, we can subtract *half of average intensity* from any points of the gray image before normalization

$$y_j = x_j - \frac{1}{2N}\sum_{j=1}^{N} x_j, \quad \vec{z} = \frac{\vec{y}}{\|\vec{y}\|} \tag{8}$$

In case of homogenous distribution on the $\mathbf{S}^N$ the scalar product of two random vectors is:

$$(\vec{w}, \vec{v}) \sim N^{-1/2} \xrightarrow{N\to\infty} 0$$

IV. SYSTEM-ON-A-CHIP (SOC)

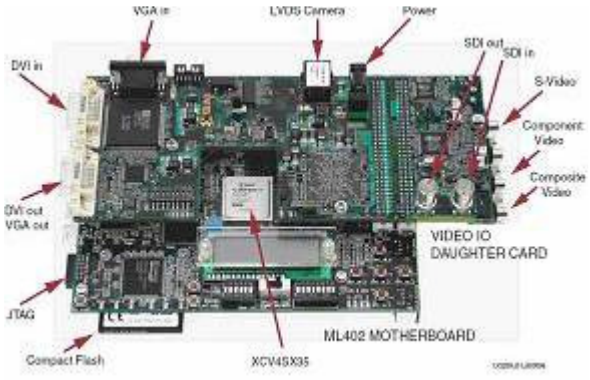

Figure 5. Xilinx ML402 development board

System-on-a-chip (SoC) refers to integrating all components into a single chip. Typically, a SoC consists of at least one processor integrated with several functionally specific hardware blocks. Using FPGA, SoC is made easy by designing custom circuits around a soft-core processor and then programmed into FPGA.

The model described in section III is implemented on Xilinx ML402 development board (Figure 10). The board consists of a Virtex4 FPGA and 64MByte DDRAM. The software development tools used are Xilinx ISE 8.2i and Xilinx EDK 8.2i. A Xilinx Microblaze softcore processor is programmed into the FPGA. Its execution codes are written in C/C++ and compiled with GNU and then loaded into the DDRAM. The Microblaze softcore processor allows additional hardware IP cores integration. The processor can pass/receive data to/from IP cores. Critical functional units are first identified and then chosen to be implemented in hardware IP core to leverage speed on parallel hardware execution.

V. EXPERIMENTAL RESULTS

Our experiment of storage and retrieval from quantum hologram are invariant face recognition for test image rotated or scaled with arbitrary angles or factors in 2D image plane.

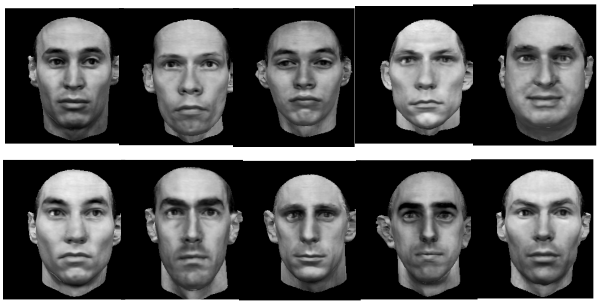

Figure 6. The ten images stored in quantum hologram

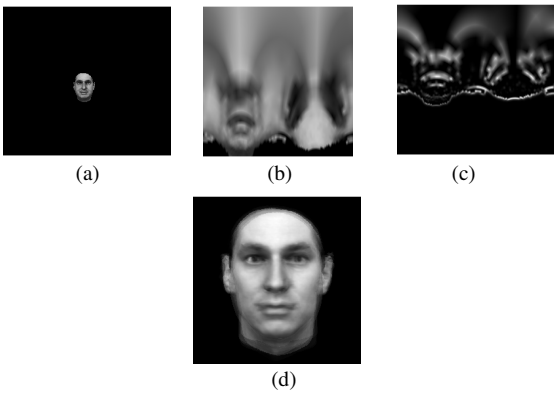

(a) (b) (c) (d)

Figure 7. (a) Scaled test image. (b) Cortical image (c) Laplacian of Gaussian image (d) Reconstructed image

The ten front-face images shown in Figure 12 are stored in the quantum hologram.

Figure 7(a) shows the reduced scale image as test image. The test image is then undergone retino-cortical mapping and projected onto the visual cortex layer (V1) as cortical image shown in Figure 7(b). Figure 7(c) depicts the result of Laplacian of Gaussian on cortical image that resembles the transformation of image along retina-LGN visual pathway. Figure (d) shows the selective reconstruction from quantum hologram trigged by the scaled image of Figure 7(a). The other experimental results are summarized in Figure 8 and Figure 9. It is evidenced that object recognition of the proposed quantum bio-inspired model is invariant to wide range of 2D rotation and scale even for the 180° inverted image.

VI. CONCLUSION

Mathematically and experimentally we showed some preliminary evidence of the 2D invariant object recognition performance of a quantum bio-inspired humanoid vision model by System-on-a-chip (SoC). Our model optimally fits experimental data and neuropsychological model – roughly at least. This paper shows how it is possible to manipulate natural quantum systems [17] to associatively process visual information in a neural-net-like way. Neuronal and dendritic nets [14] may be responsible for such hypothetical manipulation. This paper also serves as an important milestone towards the realization of physical quantum-like 'brain' for humanoid.

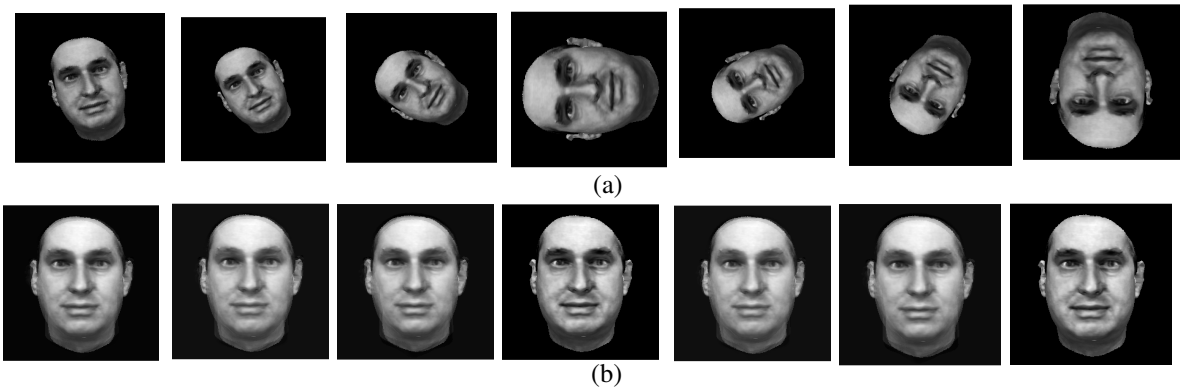

Figure 8. The rotation transformed query images. (b) The reconstructed images from quantum associative memory.

Figure 9. (a) The scale transformed query images. (b) The recalled images from quantum associative memory.

ACKNOWLEDGMENT

Authors gratefully acknowledges Ministry of Science, Technology and Innovation (Mosti), Malaysia for the eScience research Fund (03-02-01-SF0008) to support the research.

REFERENCES

[1] C. Braccini, G. Gambardella, G. Sandini, V. Tagliasco, "A model of the early stages of the human visual system: Functional and topological transformations performed in the peripheral visual field," Biological Cybernetics, vol. 44, no. 4, pp. 47-58, May 1982.

[2] H. J. Reitboeck and J. Altmann, "A model for size- and rotation-invariant pattern processing in the visual system," Biological Cybernetics, vol. 51, no. 2, pp. 113-121, Nov. 1984.

[3] G. Deco and E. T. Rolls, "A neurodynamical cortical model of visual attention and invariant object recognition," Vision Research, vol. 44, issue 6, pp. 621-642, March 2004.

[4] P. Cobos and F. Monasterio, "FPGA implementation of a log-polar algorithm for real time applications," in Dcis'99 Proc., XIV Design of circuits and integrated systems conference, 1999, pp. 63-68.

[5] C. Torres-Huitzil, B. Girau, C. Castellanos-Sánchez, "On-chip visual perception of motion: A bio-inspired connectionist model on FPGA", Neural Networks, vol. 18, pp. 557-565, Jul.-Aug. 2005.

[6] J. Ng, A. A. Bharath, Z. Li, "A survey of architecture and function of the primary visual cortex (V1)," EURASIP Journal on Applied Signal Processing, vol. 2007, pp. 124-140, Jan. 2007.

[7] T. Bolton, "General anatomy of the visual system," 2002, http://www.undergrad.ahs.uwaterloo.ca/tbolton/Anatomy.htm.

[8] P. M. Daniel, D. Whitteridge, "The representation of the visual field on the cerebral cortex in monkeys," J. Physiol., vol. 159, pp. 203-221, 1961.

[9] E. L. Schwartz, "Computational anatomy and functional architecture of striate cortex: a spatial mapping approach to perceptual coding," Vision Research, vol. 20, pp. 645-669, 1980.

[10] D. Marr and E. Hildreth, "Theory of edge detection", Proc. R. Soc. Lond. B, Biological Sciences, vol. 207, No. 1167, pp. 187-217, Feb. 1980.

[11] D. Hubel and T. Wiesel, "Receptive fields, binocular interaction and functional architecture in the cat's visual cortex," Journal of Physiology of London, vol. 160, pp. 106-154, Jan. 1962.

[12] J. G. Daugman, "Complete discrete 2-D Gabor transform by neural networks for image analysis and compression," IEEE Trans. on Acoustics, Speech, and Signal Processing, vol. 36, pp.1169-1179, Jul. 1988.

[13] S. Marcelja, "Mathematical description of the response of simple cortical cells," Journal of Optics Society America, vol. 70, no. 11, pp. 1297-1300, Nov. 1980.

[14] K. H. Pribram, Brain and Preception (Holonomy and Structure in Figural Processing). Hillsdale, NJ: Lawrence Erlbaum Associates.

[15] T. S. Lee, "Image representation using 2D Gabor wavelets," IEEE Trans. on Pattern Analysis and Machine Intelligence, vol. 18, pp. 1-13, Oct. 1996.

[16] M. S. Gazzaniga, R. Ivry, G. R.Mangun, Fundamentals of Cognitive Neuroscience, W. W. Norton, New York, NY, USA, 1998.

[17] Mijta Perus, Horst Bischof, Chu Kiong Loo, "Bio-computational model of object recognition: Quantum Hebbian Processing with Gabor Wavelets", BioSystems, 82, 116-126, 2005.

[18] P. Kruizinga, N. Petkov and S. E. Grigorescu, "Comparison of texture features based on Gabor filters," IEEE Trans. on Image Processing, vol. 11, pp. 1160-1167, Oct. 2002.

[19] M. Morrone and D. Burr, "Feature detection in human vision: a phase dependent energy model," Proc. R. Soc. Lond. B, Biological Sciences, vol. 235, no. 1280, pp. 221-245, Dec. 1988.

[20] S. Perri, M. Lanuzza, P. Corsonello, G. Cocorullo, "A high-performance fully reconfigurable FPGA-based 2D convolution processor," Microprocessors and Microsystems, vol. 29, pp. 381-391, Nov. 2005.

[21] K. Benkrid, S. Belkacemi, "Design and implementation of a 2D convolution core for video applications on FPGAs," in Proc. 3rd Int. Workshop on Digital and Computational Video, 2002, pp. 85-92.

[22] M. Z. Zhang, H. T. Ngo, A. R. Livingston, V. K. Asari, "An efficient VLSI architecture for 2-D convolution with quadrant symmetric kernels," in Proc. IEEE Computer Society Annual Symposium on VLSI, 2005,pp.303-304.